JOURNAL OF MATERIALS SCIENCE **40** (2005) 943–953

Differences in mechanical behavior between alternating and random styrene-methyl methacrylate copolymers[§]

D. RANA*, H. MOUNACH, J. L. HALARY**, L. MONNERIE
Laboratoire de Physico-Chimie Structurale et Macromoléculaire (UMR 7615), Ecole Supérieure de Physique et Chimie Industrielles de la Ville de Paris, 10 rue Vauquelin, F-75231 Paris Cedex 05, France
E-mail: jean-louis.halary@espci.fr.

The viscoelastic behavior of an alternating copolymer styrene-methyl methacrylate (S-alt-M) of composition 50:50 mol% has been investigated over a wide temperature range covering the glassy state, the glass transition region (governed by the mechanical relaxation α), and the rubbery plateau. Data were discussed by comparison with the styrene-methyl methacrylate random copolymer (S-r-M) of same composition. These studies based on tensile and shear DMTA measurements, were carried out at various temperatures and frequencies. In addition, stress-strain curves in compression mode were recorded at various temperatures and strain rates in the glassy state. The activation enthalpy and activation volume of the plastic deformation process with temperature was measured for both S-alt-M and S-r-M. Data analysis was performed on a molecular scale, by putting emphasis on the correlation existing between the amplitude of relaxation and the β-relaxation character associated to the sequence length distribution of the copolymers. From the orientation measurements of SM copolymers, carried out by infra-red dichroism, on films stretched at various gaps ($T - T_\alpha$) from the main relaxation temperature and at various strain rates, it turned out that the M segments stayed even more oriented than the S segments. Two distinct orientation relaxation curves were obtained for each type of segments, irrespective of the type of copolymer. It was shown that they could be reduced to unique ones after normalization by the zero time or zero ($T - T_\alpha$) orientation value. All these results were interpreted in relation to the role of polar-polar intermolecular interactions between M-M units, which are likely to occur in the S-r-M copolymer, but were quite lacking in the S-alt-M copolymer. However, the influence of the triad MSM on the mechanical properties was shown to progressively decrease as long as the testing temperature approaches or exceeds T_α.

1. Introduction

Conventional polystyrene (PS) and poly(methyl methacrylate) (PMMA) are known to behave differently in many respects in the solid state as well as in solution though they have monomer units very similar in volume and molecular weight and exhibit glass transition phenomenon in the same temperature range. For example, the molecular weight between entanglements of PS is roughly twice as that of PMMA.

During the past decades, some research in this laboratory has focused on viscoelastic, orientation, and relaxation behavior of styrene-methyl methacrylate random copolymers (S-r-M) [1–3]; viscoelastic and mechanical properties of methyl methacrylate-based random copolymers [3–6]; viscoelastic, orientation and relaxation behavior of PMMA and PS homopolymers [7–10].

In the recent literature, there are some interesting results regarding the relationship between copolymer sequence length distributions (i.e., arrangement of comonomers) and their properties [11–14]. Suzuki *et al.* proved that the distribution of the length of the sequence and also tacticity in SM copolymers influenced the glass transition temperature (T_g) [11, 12]. Galvin and coworkers showed that an alternating distribution of SM copolymers leads to an improved miscibility with PMMA compared to that of the random SM copolymers [13, 14].

[§]This article is dedicated to the memory of Dr. Bruno JASSE, at the approach of the tenth anniversary of his decease in November 1995.
*Present address: Dept of Chemical Engineering, University of Ottawa, 161 Louis Pasteur St., Ottawa, Ontario, K1N 6N5, Canada
**Author to whom correspondence should be addressed.

The purpose of the present study is to report on the viscoelastic behavior, plastic deformation, orientation and orientation relaxation behaviors of an alternating styrene-methyl methacrylate copolymer (S-alt-M) of composition 50:50 mol%. Our objective is to compare these new data to those already published for styrene-methyl methacrylate random copolymers (S-r-M) and in particular for that of same comonomer content as the alternating copolymer. This approach should help in clarifying the influence on mechanical properties of S-M copolymers of the presence of MSM triads, which are supposed to be the unique linkings in S-alt-M, but on the other hand are much less abundant in S-r-M copolymers.

2. Experimental

2.1. Materials

The styrene-methyl methacrylate alternating copolymer (S-alt-M), 50 mole% of M, was obtained by copolymerization of styrene and methyl methacrylate monomers in the toluene medium using ethyl aluminium sesquichloride as the catalyst [15]. In order to remove the low molecular weight chains, the samples were purified by precipitation in methanol from a chloroform solution. Then, they were dried in a vacuum oven at 40°C to remove most of the solvent, and finally dried at 150°C for 24 h.

The alternating character of the monomer sequence distribution of the S-alt-M sample has been checked using carbon-13 nuclear magnetic resonance spectroscopy (NMR). As expected, the spectra (not shown) obtained from $CDCl_3$ solutions using a Bruker AC 200 spectrometer operated at 50 MHz and 25°C does not reveal the presence of M-M and S-S linkings.

The weight average molecular weight (M_w), number average molecular weight (M_n), and polydispersity index ($I = M_w/M_n$), were measured by gel permeation chromatography (GPC). The glass transition temperature T_g was obtained using a TA differential scanning calorimeter (DSC) at a heating rate of 10°C min^{-1}. The thermal and molecular weight characteristics of the S-alt-M copolymer are listed in Table I. The characteristics of the copolymer S-r-M, which will be used for sake of comparison, are also recalled in Table I; they have been taken from reference [1]. The T_g of S-alt-M is slightly lower compared to the S-r-M, as already observed by Suzuki *et al.* [11].

Within the framework of our studies, other important features of the copolymers S-alt-M and S-r-M are their configurational and conformational states. Tacticities were determined according to the proton and carbon-13 NMR methods available in the literature [16, 17]. The relevant amounts of triads mm (isotactic), rr (syndiotactic) and mr (heterotactic) are given in Table II for both S-alt-M and S-r-M 50:50 copolymers. The overall amount of trans-trans conformations in both samples was deduced from the analysis of the infrared spectra in the region 500–600 cm^{-1}, as detailed in reference [2]. Data given in Table II show the drop in trans-trans conformations from S-r-M to S-alt-M. This result has been mainly justified by the disappearance of SSM linkings in S-alt-M [18].

TABLE I Main characteristics of the SM copolymers under study

Sample	M_w (kg mol^{-1})	M_n (kg mol^{-1})	I (M_w/M_n)	T_g(DSC) (°C)
S-alt-M 50:50 mol%	375	120	3.12	103
S-r-M 50:50 mol%	140	70	2.00	106

TABLE II Configurational and conformational characteristics of the SM copolymers

Sample	Triads mm (%)	Triads rr (%)	Triads mr (%)	Overall % of trans-trans conformations
S-alt-M 50:50 mol%	24	19	57	3
S-r-M 50:50 mol%	17	34	49	42

2.2. Viscoelastic measurement conditions

The viscoelastic properties of the sample S-alt-M were investigated over an extended temperature range covering the glassy state, the glass transition region, the rubbery plateau, and the terminal zone by using complementary testing systems. Test conditions were chosen in such a way that the observed behavior strictly obeys the laws of linear viscoelasticity.

A dynamic mechanical analyzer DuPont DMA 983 was used to explore temperatures ranging from −150°C to $T_g + 10$°C and frequencies ranging from 0.1 Hz to 3 Hz. The applied strain was 0.15% in flexural mode. The flexural data were transformed into E' and E'' by using a routine available on the DMA and by taking a Poisson ratio, averaged to 0.40 on the temperature range under consideration.

The α relaxation region was investigated using a servo-hydraulic testing machine MTS 831-10 which was operated in a tensile mode. Twelve driving frequencies per decade were chosen over the range 0.01 to 80 Hz. The samples were subjected to a static strain of about 0.1% on which was superimposed a sinusoidal strain varying from −0.05% to +0.05%. The temperature increment between successive measurements was 2°C. A routine available with the instrumentation calculated the values of tensile storage modulus (E'), tensile loss modulus (E''), and the damping tan $\delta(= E''/E')$ from the experimental values of stiffness and phase angle δ. The measurements were performed from −85°C to 120°C.

The rubbery plateau and terminal zones were investigated by oscillatory shear experiments performed on a Weissenberg-type rheometer (Rheometrics RDA II) operated in parallel-plate geometry. The driving angular frequencies covered the range 0.01 rad s^{-1}–100 rad s^{-1}. Strain was varied from 1% in the plateau region up to 7% in the terminal zone according to the signal obtained. Computer processing of the experimental measurements yielded shear storage modulus (G'), loss modulus (G''), and tan $\delta = G''/G'$. The geometry of the samples was dictated by the characteristics of the testing machine. Bars of $10 \times 60 \times 2$ mm^3 were used for DMA.

Bars ($60 \times 12 \times 3$ mm^3), and disks (25 mm in diameter and 1.6 mm thickness) were used with the MTS testing system, and the Rheometrics equipment, respectively. In order to eliminate water which might be associated with the carbonyl group, all samples were compression molded in vacuum at 160°C and then quenched down to room temperature.

2.3. Viscoelastic data analysis

One could refer for instance to references [1] and [10] for more details on the data analysis procedure summarized below.

In the secondary relaxation region, the frequency dependence of the maximum of the E'' peak was analyzed according to the Arrhenius equation:

$$\log_{10} \frac{\nu_T}{\nu_{T_0}} = \frac{Ea}{2.3R}\left(\frac{1}{T_0} - \frac{1}{T}\right) \tag{1}$$

In the glass transition region, according to the frequency-temperature superposition principle [19], the curves of E' (or E'') versus frequencies can be reduced to a unique master curve at an arbitrarily chosen reference temperature, T_0, provided appropriate horizontal shifts of $\log a_{T/T_0}$ (often denoted $\log a_T$ for simplicity) are made along frequency scale. No vertical shift was applied, considering the change of density negligible over the temperature range under consideration. The temperature dependence of the shift factor is expected to obey the Williams-Landel-Ferry (WLF) type equation:

$$\log a_T = -\frac{C_1^0(T - T_0)}{C_2^0 + T - T_0} \tag{2}$$

which can be rewritten in the form:

$$\frac{T - T_0}{\log a_T} = -\frac{T - T_0}{C_1^0} - \frac{C_2^0}{C_1^0} \tag{3}$$

where C_1^0 and C_2^0 denote the viscoelastic coefficients at the temperature T_0.

The consistency of the experiments can be checked easily by plotting the $(T - T_0)/\log a_T$ versus $(T - T_0)$: the values of a_T extracted from the construction of both E' and E'' master curves do lead to a unique linear plot. This behavior is actually observed for each frequency, provided experimental data for temperatures below the maximum of E'' are disregarded. Data with $T - T_0 < 5$°C are also neglected, because too large uncertainties affect the quantity $(T - T_0)/\log a_T$. The values of viscoelastic coefficients C_1^0 and C_2^0 can be derived from the slope and intercept with the Y axis of the straight line. With a view to compare different materials, values of the viscoelastic coefficients C_1^g and C_2^g were determined systematically at T_α (1 Hz), taken as the reference temperature and identified to T_g. This is achieved using:

$$C_1^g C_2^g = C_1^0 C_2^0 \tag{4}$$

$$\text{and } T_g - C_2^g = T_0 - C_2^0 = T_{inf} \tag{5}$$

T_{inf} is the temperature at which the cooperative motions involved in the glass transition would appear at infinitely low driving frequency.

The molecular meaning of the coefficients C_1^g and C_2^g could be extracted from the well-known equations attached to the free volume theory [19], namely the Doolittle equation [20] and the thermal expansion coefficient of the free volume above T_g. The following relations hold:

$$C_1^g = \frac{B}{2.3 f_g} \tag{6}$$

and

$$C_2^g = \frac{f_g}{\alpha_f} \tag{7}$$

where f_g is the fractional free volume available at T_g and α_f is the free volume expansion coefficient above T_g. B is an empirical constant in the Doolittle equation and is usually assumed to be unity.

One of the most important parameters in the rubbery zone is the pseudo-equilibrium modulus of the entanglement network G_n^0, which can be related to the average molecular weight between coupling loci, M_e, through the relation [19]:

$$G_n^0 = \frac{g\rho RT}{M_e} \tag{8}$$

where g is a numerical factor assumed to be unity, ρ is the density, and R is the gas constant. G_n^0 may be determined for instance as the storage modulus G' at the frequency where $\tan\delta$ is at its minimum in the plateau zone. According to Wu, one can calculate the number of real skeletal bonds N_e in an entanglement strand by the formula [21]:

$$N_e = n_r \frac{M_e}{M_r} \tag{9}$$

where n_r and M_r are the number of skeletal bonds in a repeat unit (in the present case, $n_r = 2$) and the molecular weight of repeat unit, respectively.

In the region where G' equals G'' and both quantities depend on the square root of frequency, the monomeric friction coefficient, ζ_{oT}, can be extracted from the Rouse equation [19]:

$$G' = G'' = \frac{a\rho N_A}{4M_o}\left(\frac{\zeta_{oT} kT}{3}\right)^{1/2} \omega^{1/2} \tag{10}$$

where ρ is the density, N_A is the Avogadro number, M_o is the monomer molecular weight, k is the Boltzmann constant, ω is the frequency, and a is the characteristic

length which is defined as:

$$a = \left(\frac{r_o^2}{M_n}\right)^{1/2} M_o^{1/2} \tag{11}$$

As a is unknown for most of the copolymers (and especially for the SM copolymers), it is usual to take a value averaged from those of the parent homopolymers. In our case, the available values of $(\frac{r_o^2}{M_n})^{1/2}$ are $(640 \pm 60)\ 10^{-4}$ nm.kg$^{-1/2}$ and $(670 \pm 60)\ 10^{-4}$ nm.kg$^{-1/2}$ for conventional PMMA and PS, respectively [22, 23].

From ζ_{oT}, calculated at the reference temperature T, the intrinsic monomeric friction coefficient, ζ_{oo}, (relative to the reference temperature T_{inf}) was finally deduced using the Vogel relation [19]:

$$\ln \zeta_{oT} = \ln \zeta_{oo} + \frac{1}{\alpha_f (T - T_{inf})} = \ln \zeta_{oo} + 2.3 C_1^T \tag{12}$$

2.4. Plastic deformation measurements

Plasticity measurements were carried out in compression mode on a servo-hydraulic testing machine MTS 810 within a range of temperature −75°C to 80°C and strain rate over the range 2×10^{-1}s^{-1}–2×10^{-4}s^{-1}. The compression test specimens of size $3 \times 3 \times 5$ mm^3 were cut with a diamond knife using a Krautkramer Isomet low speed saw.

For the yield stress, σ_y, calculation was done by the maximum stress, and for the plastic flow stress, σ_{pf}, was considered as the minimum stress of the stress-strain compression curves which lead to plastic consolidation. The softening amplitude, SA, was estimated from the difference between the yield stress and plastic flow stress, $SA = \sigma_y - \sigma_{pf}$. Yield stress, plastic flow stress, and softening amplitude were calculated from curves as the average on three to five samples.

The activation volume of the plastic deformation process, V_o, and its activation enthalpy, ΔH_o, can be calculated using the equations [24–27]:

$$V_o = RT\left(\frac{d \ln \dot{\varepsilon}}{d\sigma_y}\right)_T \tag{13}$$

$$\text{and } \Delta H_o = -T V_o \left(\frac{d\sigma_y}{dT}\right)_{\dot{\varepsilon}} \tag{14}$$

where $\dot{\varepsilon}$ is the strain rate.

Basically, V_o is an index of the sensitivity of the plastic deformation to strain rate, which is calculated from the slope of the plots of yield stress versus logarithmic of strain rate. All measurements were performed on samples subjected to the same thermal history in order to satisfy the required isothermal conditions.

2.5. Orientation measurements

Thin films suitable for infrared spectroscopy were obtained by casting a 6% chloroform solution on a glass plate. Subsequent annealing was done under vacuum above T_g, in order to remove any trace of solvent and residual stresses. Oriented samples from thin films were obtained on an apparatus developed in our laboratory, i.e., a stretching machine operating at constant strain rate and equipped with a special oven designed to get a very good thermal stability over the entire sample (homogeneity is ca. 0.2°C). Draw ratios were measured using ink marks on the sample. Under these conditions, the degree of crystallinity of the samples is essentially zero, as checked by DSC measurements. The samples were stretched at five different temperatures over the range 5.5 K $\leq T - T_\alpha \leq$ 17.5 K and three different strain rates (0.115, 0.026, 0.008 s^{-1}). The polarized spectra were recorded using a 7199, or a 205 Nicolet Fourier transform infrared spectrometer. A gold wire-grid Specac polarizer, set at a maximum transmission position, was used and the samples rather than the polarizer were rotated 90° in order to obtain the two polarization measurements. A total at 100 co-added interferograms were scanned at 2 cm^{-1} resolution. The infrared dichroism, R, was calculated as $R = A_\parallel / A_\perp$ for the peak absorbances $A_\parallel$ and $A_\perp$. Self-deconvolution and curve analysis were realized using the Nicolet software provided with the spectrometers. Dichroic ratio measurements yield the second-order moment of the orientation function according to the relations [28]:

$$\langle P_2(\cos\theta)\rangle = \frac{1}{2}\left(3 < \cos^2\theta > -1\right) = \frac{R-1}{R+2}\frac{R_o+2}{R_o-1} \tag{15}$$

where θ is the angle between the chain axis and the draw direction, and

$$R_o = 2\cot^2\alpha \tag{16}$$

where α is the angle between the chain axis and the dipole moment vector of the considered vibration. Choice of suitable bands was made according to the earlier results of our laboratory on the orientation of PMMA and S-r-MMA copolymer chains [2, 10]. The orientation of the styrene segments, $\langle P_2(\cos\theta)\rangle_S$, was measured from the dichroism of the 1028 cm^{-1} absorption band, which appears in a window of the PMMA spectrum. This band corresponds to the in plane ν_{18a} mode of the benzene ring and makes an angle $\alpha = 90°$ with respect to the chain axis. As far as the MMA segments are concerned, no absorption band is absolutely free of any contribution from the S segments. In fact, $\langle P_2(\cos\theta)\rangle_{MMA}$ was measured from the dichroism of the 1388 cm^{-1} band, which is assigned to the C-CH$_3$ symmetrical bending vibration, whose dipole moment vector is roughly perpendicular to the chain axis. It has been shown [2] that some overlapping of this band with the styrene band located at 1375 cm^{-1} results in a slight underestimation of $\langle P_2(\cos\theta)\rangle_{MMA}$ but this effect will be neglected, as a first approximation, in our data analysis.

The dichroism measurements were taken on three samples stretched in the same temperature and strain rate conditions at a draw ratio of $\lambda = 3$. These results were then extrapolated to $\lambda = 4$, the orientation function

$\langle P_2(\cos\theta)\rangle$ being taken as a linear function of λ in these experimental conditions.

2.6. Orientation relaxation measurements

The measurements on the S-alt-M were done for different relaxation times, t_R, between 0 to $3.2 \cdot 10^3$ s on samples stretched in the conditions: $(T - T\alpha) = 11.5°C$ and $\dot{\varepsilon} = 0.115\ s^{-1}$. With the goal of comparing the relaxation of the two types of segments M and S, normalized relaxation curves were drawn by considering the time dependence of the ratio $\Re_1$ of $\langle P_2(\cos\theta)\rangle_{t_R}$ at time t_R to $\langle P_2(\cos\theta)\rangle_o$ at initial orientation. Alternatively, other normalized relaxation curves were drawn by considering the temperature dependence of the ratio $\Re_2$ of $\langle P_2(\cos\theta)\rangle(T - T_\alpha)$ at given gap $(T - T_\alpha)$ to $\langle P_2(\cos\theta)\rangle_{5.5K}$ at the lower gap under consideration, i.e. 5.5 K.

3. Results and discussion

3.1. The β relaxation

The loss modulus traces E'' (1 Hz) of alternating and random SM copolymers are compared in Fig. 1 over the temperature range −85°C to 40°C. As already known [29], S-r-M presents a well-defined broad peak in the secondary relaxation region. S-alt-M presents the same behavior as S-r-M in the high temperature part of the relaxation. Analysis of the frequency dependence of the β relaxation maximum leads to the Arrhenius plots of $\log_{10}\nu$ versus reciprocal temperature, 1/T, given in Fig. 2. The activation energies, E_a, deduced from the slope of these plots according to Equation 1 are very close to each other for S-alt-M and S-r-M, namely 48.5 kJ mol^{-1} for the former and 52.5 kJ mol^{-1} for the latter. However, as a noticeable peculiarity, S-alt-M also exhibits a strong and continuous damping at low temperature.

The molecular nature of the PMMA β relaxation has been examined by NMR [29]. At this occasion, it has been shown that the motions responsible for this process couple a 180° rotation of the O—C═O lateral group and a main-chain torsion of ca 20° around the local chain axis. In the copolymers, it is reasonable assuming that the insertion of S units between two M units is likely to facilitate the movement possibilities of the ester groups, and, in turn, of the coupled MMA main chain torsions, by screening the dipolar interactions between ester groups. This effect is expected to be important in S-alt-M, where all linkings are of SMS type, and much less pronounced in S-r-M, where substantial amounts of MMS and even MMM type linkings are present. This explanation is consistent by the earlier observations of Muzeau *et al.* [30] on S-r-M copolymers of variable S content: these authors observed that the temperature of the maximum of MMA β damping ($\tan\delta$) decreases with increasing styrene content. The progressive 'dilution' of the MMA units along the chain would also reduce the probability for MMS and MMM sequences, and therefore enhance the screening of MMA dipolar interactions and render the low temperature β motions much easier. Another (complementary) explanation for the low temperature damping in S-alt-M can be found in the lack of trans-trans conformations (Table II): the correlative increase in trans-gauche and gauche-gauche conformations, indeed, would be likely to favor the ester group mobility, as detailed elsewhere [18].

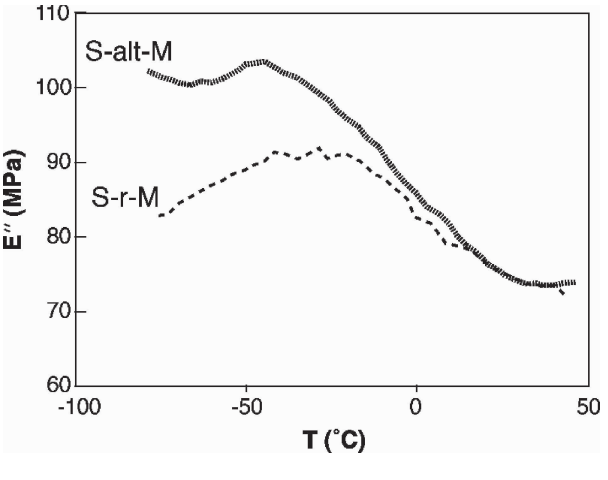

Figure 1 Dependence of tensile loss modulus (E'') versus temperature at the frequency 1.58 Hz.

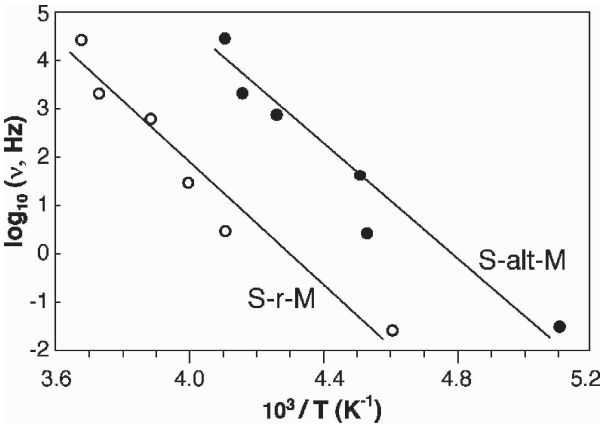

Figure 2 $\text{Log}_{10}(\nu, \text{Hz})$] versus reciprocal temperature (K^{-1}) in the β relaxation region for S-alt-M (●) and S-r-M (○).

3.2. The α relaxation region

Let us consider now the viscoelastic data collected over the temperature range 80–120°C, i.e. the range where the glass transition phenomena are likely to find a mechanical expression. Fig. 3 shows the temperature dependence of the tensile storage modulus, E', loss modulus, E'', and $\tan\delta$ for the S-alt-M copolymer at the frequency 1 Hz. All the plots clearly account for the occurrence of the main relaxation α, conventionally characterized by the temperature, $T\alpha$ (1 Hz), corresponding to the maximum of the E'' peak. The frequency dependence of E' and E'' at various fixed temperatures is shown in Fig. 4. Accurate master curves (not shown) can be built from these data, and quantitative analysis of the relevant shift factors a_T according to Equation 2 (Fig. 5) yields the values of C_1^g and C_2^g, and then of $T_{inf} = T\alpha$ (1 Hz) $- C_2^g$ according to Equation 5. All the above viscoelastic characteristics relative to the S-alt-M sample are grouped in Table III,

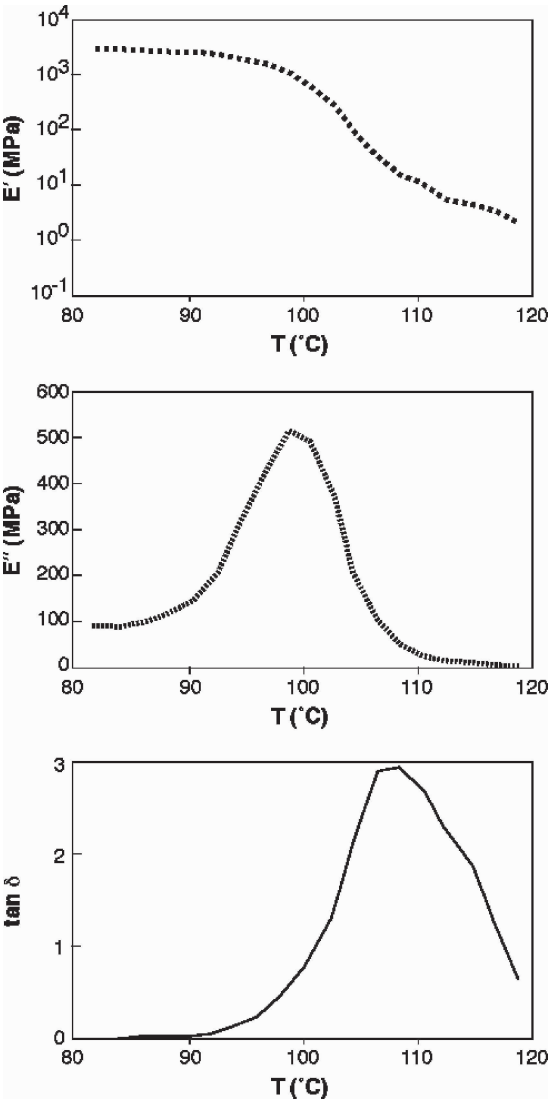

Figure 3 Variation of tensile storage modulus (E'), loss modulus (E''), and damping tan δ measured at 1 Hz versus temperature for the S-alt-M.

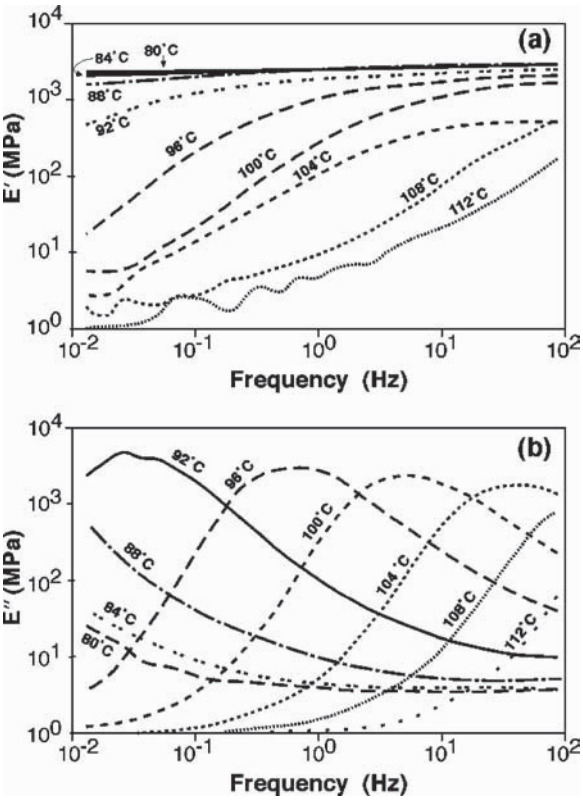

Figure 4 Tensile storage modulus (E') [plot a] and loss modulus (E'') [plot b] versus frequency (ν, Hz) for the S-alt-M at various temperatures (°C).

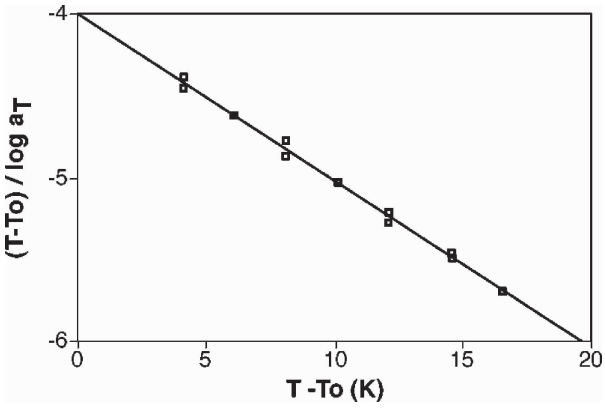

Figure 5 Analytic determination of the viscoelastic coefficients C_1^0 and C_2^0 from the values of the shift factors a_T for the S-alt-M copolymer at the reference temperature $T_0 = 100°C$.

together with those relative to S-r-M, given for sake of comparison.

It has been recognized for years that T_g (10°C·mn^{-1}) and $T\alpha$ (1 Hz) present values very close to each other for many polymers. Tables I and III show that this assessment is quite well verified by both S-alt-M and S-r-M copolymers. More interesting is to notice that S-alt-M exhibits a slightly lower T_g (respectively, T_α (1 Hz)) than S-r-M. This could be justified by two arguments: first, the lack of polar interactions in S-alt-M (already discussed in the previous paragraph), which increases the chain mobility; and secondly, the configurational structure of the chains. It is known, indeed, that for both polystyrene and PMMA homopolymers, T_g increases with the increase in the number of syndiotactic triads [22]. As S-alt-M possesses much less syndiotactic rr triads and more isotactic mm triads than S-r-M (Table II), then its T_g would be lower.

The criterion of higher mobility for S-alt-M as compared to S-r-M also affects the values of the fractional free volume available at T_α (1 Hz), f_g, and of the free volume expansion coefficient above T_α (1 Hz), α_f, (Table III): as expected, both quantities increase from S-r-M to S-alt-M.

TABLE III Viscoelastic characteristics of the SM copolymers in the glass transition region

Sample	T_α (1 Hz) (°C)	C_1^g	C_2^g (°C)	T_{inf} (°C)	$10^2\ f_g/B$ (%)	$10^4\ \alpha_f/B$ (°C^{-1})
S-alt-M	99	10.9	35.0	64.0	3.98	11.38
S-r-M	103	11.9	36.5	66.5	3.65	9.99

3.3. The deformation behavior below T_α

Examples of the experimental stress-strain curves obtained either at variable temperature and constant strain rate or at fixed temperature and variable strain rate are

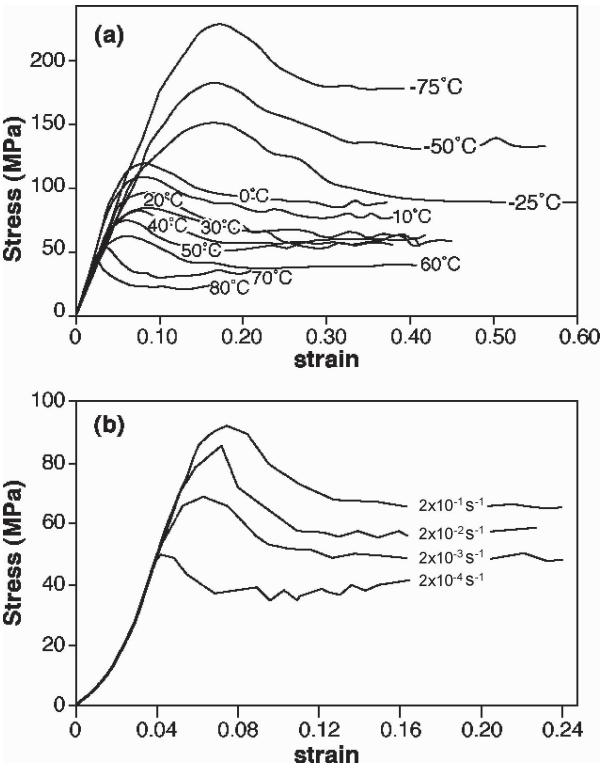

Figure 6 Typical stress-strain curves of the SM 50:50 copolymers: (Plot a): temperature effect for the sample S-r-M at a constant strain rate $\dot{\varepsilon} = 210^{-2}\ s^{-1}$; (Plot b): strain rate effect for the sample S-alt-M at a temperature of 60°C.

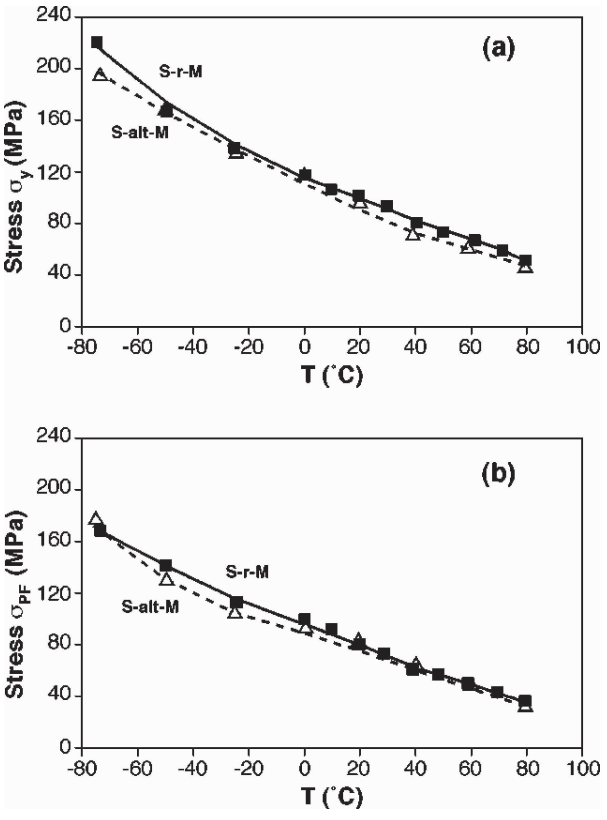

Figure 7 Yield stress,σ_y, and plastic flow stress, σ_{PF}, temperature profiles at a strain rate $\dot{\varepsilon} = 210^{-3}\ s^{-1}$s for the S-alt-M (△) and S-r-M (■) copolymers. (Plot a): yield stress; (Plot b): plastic flow stress.

shown in Fig. 6. Our set of data relative to the S-r-M 50:50 copolymer are in quite good agreement with those already published by Gloaguen *et al.* [31]. The plot of yield stress, σ_y, versus temperature and plastic flow stress, σ_{pf}, versus temperature at the regular strain rate of $2{\cdot}10^{-3}s^{-1}$ are shown for both S-alt-M and S-r-M samples in Fig. 7a and b, respectively. These results can be discussed in relation to the lines of molecular reasoning well established in recent publications [5, 6, 33–36]. The molecular motions involved in plastic flow are the same as those concerned by the α relaxation: it is therefore not surprising that σ_{pf} temperature profiles are roughly identical for S-alt-M and S-r-M. The molecular motions involved at the yield point are the same as those concerned by the β relaxation at the temperature of interest: in the higher part of the relaxation, S-alt-M and S-r-M present roughly the same σ_y profile as they present the same β relaxation profile (Fig. 1); on the other hand, in the lower part of the relaxation, S-alt-M exhibits more damping than S-r-M, which explains the larger facility of the former to attain the yield at lower cost, i.e. at a slightly lower σ_y value. In polystyrene, the softening amplitude $SA = \sigma_y - \sigma_{pf}$ is large because the β motions are poor plasticity promoters as compared to the α ones; by contrast, *SA* tends to vanish for PMMA at sufficiently high temperature, because the β motions are quite similar to the α motions (α-precursors) [6]. In the case of the SM copolymers (Fig. 8), *SA* is quite large since the β motions tend to be decoupled from the α ones. As expected, *SA* is lower for S-alt-M than for S-r-M at low temperature, and the reverse trend is observed on the high temperature edge, because of a better decoupling of α and β motions.

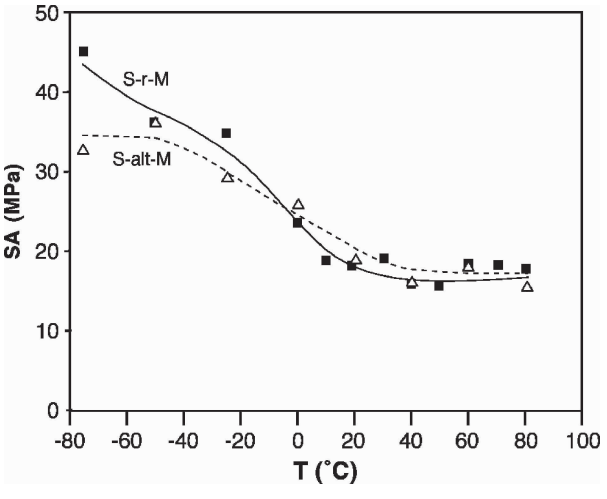

Figure 8 Strain softening versus temperature for the SM 50-50 copolymers at the strain rate $\dot{\varepsilon} = 210^{-3}s^{-1}$: (△) S-alt-M;(■) S-r-M.

Following the approach developed for instance by Lefebvre *et al.* [25–27, 31], another way to provide a molecular analysis of the plasticity phenomena is to consider the strain rate dependence of σ_y (Equations 13 and 14). Fig. 9a and b show the temperature dependence of the activation volume, V_o, and of the activation enthalpy, ΔH_o, respectively. For both SM copolymers, the V_o and ΔH_o values increase with increasing temperature. Because of a better precision on the measurements, V_o is the more suitable quantity to be discussed for comparison purpose. The larger values observed for

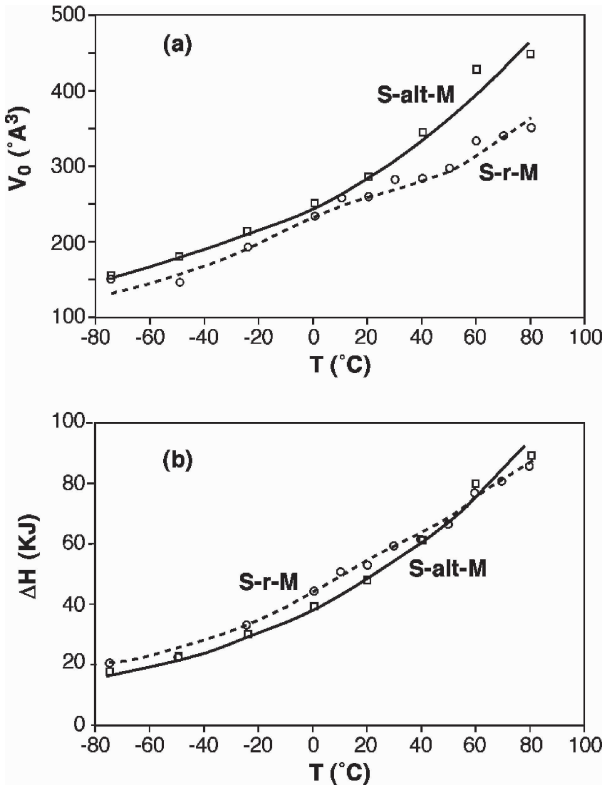

Figure 9 Plastic deformation activation parameters versus temperature for the S-alt-M (□) and S-r-M (○) copolymers. (Plot a): activation volume V_o; (Plot b) activation enthalpy ΔH_o.

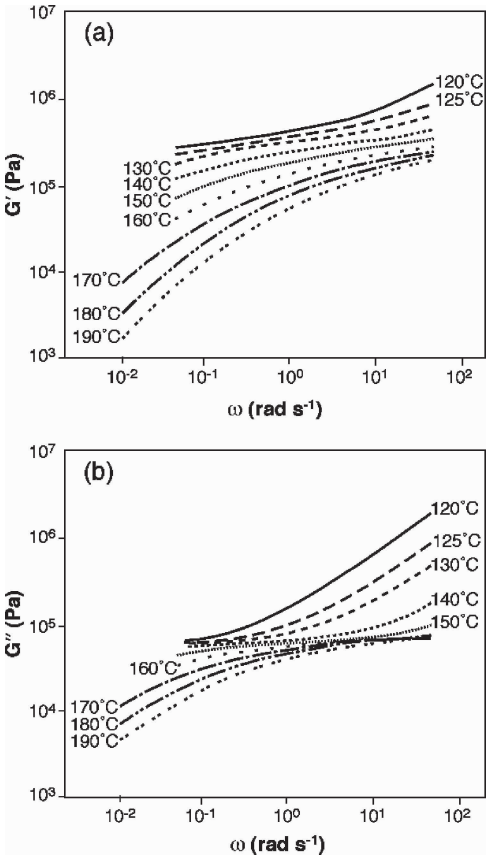

Figure 10 Variation of (a) shear storage modulus (G′), and (b) loss modulus (G'') versus angular frequencies (ω, rad s^{-1}) for the S-alt-M copolymer at various temperatures (°C).

S-alt-M may be understood, at least in the lower temperature range, again as in index of easier development of sheared micro-domains in relation to the presence of more numerous mobility sites.

3.4. The viscoelastic behavior above T_α

In Fig. 10, the shear storage modulus, G', and the loss modulus, G'', at various temperatures are plotted logarithmically against the angular frequency, ω, for the S-alt-M copolymer. Such curves of G' and G'' versus log ω as well as similar curves for the dynamic viscosity, η', at various temperatures can be superimposed into master curves by use of the time-temperature superposition principle, as described above. As an illustration, Fig. 11 gives the master curve of G', G'', and η' of the S-alt-M at the reference temperature $T_0 = 140$°C. By following the same procedure as described in paragraph 3.2, an attempt has been made to evaluate the values of C_1^0 and C_2^0 at the reference temperature T_0, then to derive from equations 4 and 5 the values of C_1^g and C_2^g at the reference temperature T_α, and finally to compare theses values determined in the E' transient plateau range to those above derived in the E'' maximum range. Such a procedure has given reliable results for S-r-M [1]. For reasons not understood yet, it does not work satisfactorily with S-alt-M data, which yield appreciable discrepancies, as tentatively discussed in reference [18]. Below, we will just consider the values given in Table III.

The molecular weight between entanglements, M_e, of S-alt-M has been derived from the viscoelastic data by using the Equation 8, and the number of real skeletal bonds in an entanglement strand, N_e, has been derived from Equation 9. For sake of consistency with the S-r-M case, for which the value of M_e has already been published [1], the same density $\rho = 1095$ kg·m^{-3}, i.e. the average value of the densities of PMMA (1150 kg·m^{-3}) and PS (1040 kg·m^{-3}) [22], has been taken for the calculations. The values of G_n^0, M_e, and N_e are given in Table IV for both S-alt-M and S-r-M. One may consider that the S-alt-M chains are slightly less entangled than the S-r-M chains, as the result of a more pronounced dynamic flexibility. Their reduced number of trans trans conformations at the benefit of

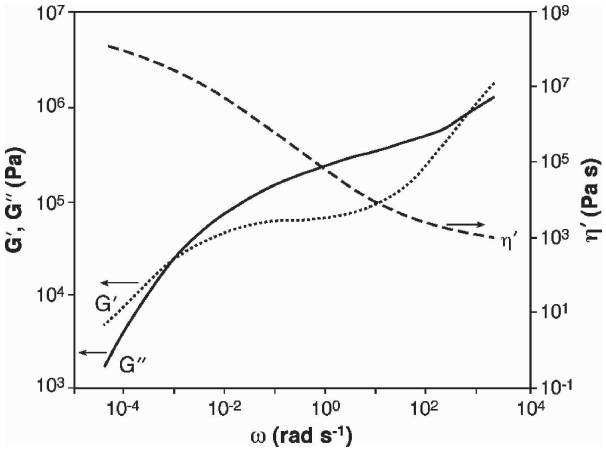

Figure 11 Master curves of shear storage modulus (G'), loss modulus (G''), and dynamic viscosity (η') versus angular frequencies (ω, rad s^{-1}) for the S-alt-M copolymer at the reference temperature $T = 140$°C.

TABLE IV Rheological characteristics of SM copolymers in the plateau region

Sample	$10^{-5}G_n^0$ (N m^{-2})	M_e (kg mol^{-1})	N_e
S-alt-M	2.84	13	255
S-r-M*	3.30	11.5	225

*Data taken from reference [1].

TABLE V Monomeric friction coefficient (N s m^{-1}) of SM copolymers

Sample	$10^{-3}\ln\zeta_{oT}$ at 140°C	$10^{-3}\ln\zeta_{oo}$ at T_{inf}
S-alt-M	−7.73	−19.29
S-r-M*	−7.28	−20.87

*Data taken from reference [1].

trans gauche and gauche gauche conformations may be once more invoked to justify this feature.

Finally, the monomeric friction coefficients, which characterize the resistance encountered by the monomer units to move through their surroundings, are given in Table V. The values relative to S-alt-M have been calculated from the viscoelastic data of the present study by using the Equations 10–12, those relative to S-r-M have been taken from the literature [1]. One should point out that the uncertainties on the values of $\ln\zeta_{oT}$ and mostly of $\ln\zeta_{oo}$ are quite large: typically, the error bar on $\ln\zeta_{oo}$ can be estimated to ± 1.4. Therefore, ζ_{oo} values given in Table V should be regarded as identical for S-alt-M and S-r-M and not discussed further.

3.5. The chain orientation and relaxation above T_α

For S-alt-M, the second-order moments of the orientation function, respectively $\langle P_2(\cos\theta)\rangle_{MMA}$ for the MMA segments and $\langle P_2(\cos\theta)\rangle_S$ for the styrene segments, are given in Fig. 12. Whatever these quantities are plotted as a function of the temperature gap $(T - T_\alpha)$ (Fig. 12a) or as a function of reciprocal strain rate (Fig. 12b), the effects of the competition between orientation and orientation relaxation are obvious: the greater the chain mobility, the lower the measured orientation is. More important is to note that, for any stretching condition, S and M segments orientations are different, M segments being always more oriented than S segments. Chain relaxation effects can be visualized by plotting $\langle P_2(\cos\theta)\rangle_{MMA}$ and $\langle P_2(\cos\theta)\rangle_S$ as a function of the experimental relaxation time t_R (Fig. 13a): in absolute, the M segments relax much faster than the S segments. It is interesting to compare the relaxation of the two kinds of segments by considering the relaxation function $\Re_1$, corresponding to the normalization of the orientation function at time t_R by the initial orientation function. The results, given in Fig. 13b, show that in spite of a certain dispersion of the data points, the two segments have a similar orientation relaxation profile. They are corroborated, with a much greater accuracy, by plotting as a function of $(T - T_\alpha)$ (Fig. 14) the relaxation function

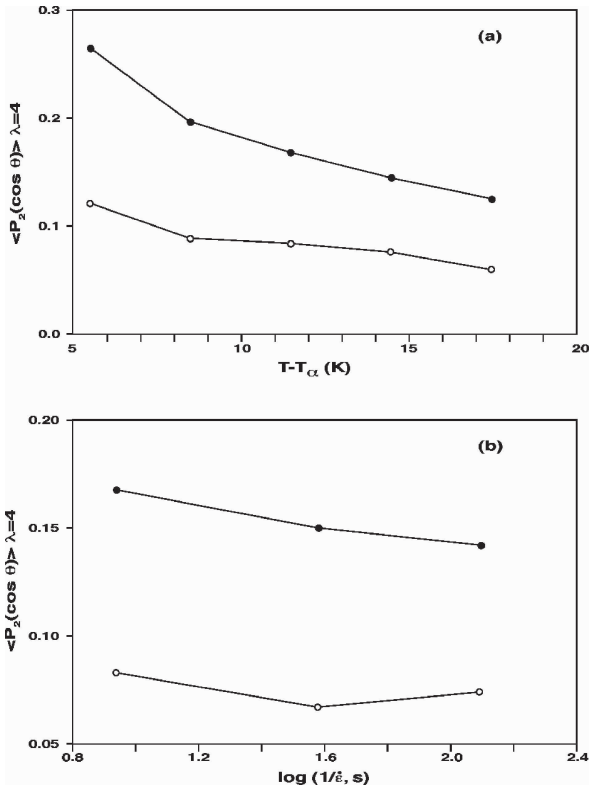

Figure 12 Orientation of the M (●) and S segments (○) of the S-alt-M copolymer. (Plot a): influence of stretching temperature at the strain rate $\dot{\varepsilon} = 0.115\ s^{-1}$; (Plot b): influence of strain rate at the reference temperature such that $T - T_\alpha = 11.5$ K.

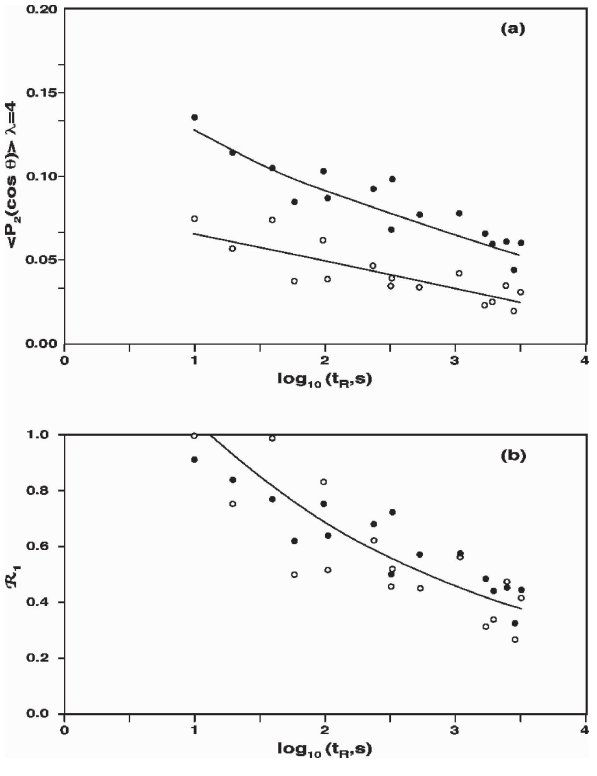

Figure 13 Orientation relaxation of the M (●) and S segments (○) of a S-alt-M sample pre-strained till $\lambda = 4$ at a reference temperature such that $T - T_\alpha = 11.5$°C and at a strain rate $\dot{\varepsilon} = 0.115\ s^{-1}$. (Plot a): $\langle P_2(\cos\theta)\rangle$ versus relaxation time; (Plot b) $\Re_1$ versus time.

$\Re_2$, corresponding to the normalization of the orientation function at gap $(T - T_\alpha)$ by the orientation function relative to the lowest gap available (5.5 K). From a qualitative viewpoint, the above described orientation and

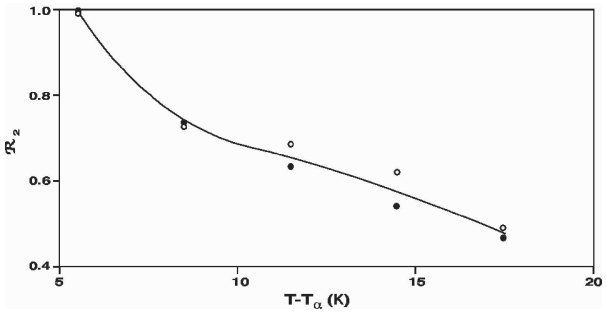

Figure 14 Orientation relaxation of the M (●) and S segments (○) of a S-alt-M sample pre-strained till $\lambda = 4$ at a strain rate $\dot{\varepsilon} = 0.115\ s^{-1}$: master curve of $\Re 2$ versus $T - T_\alpha$.

orientation relaxation behavior of S-alt-M is identical to that previously reported for the S-r-M 50:50 copolymer [2]: in comparable stretching conditions, MMA segments orientation is larger than S segments orientation. In addition, S units orient more readily in S-r-M than in polystyrene homopolymer, as they are influenced by the neighborhood of MMA units [7]. Direct comparison of the behavior of S-alt-M and S-r-M is facilitated by the fact that both samples present the same monomeric friction coefficients, which allows unquestionably the $(T - T_\alpha)$ scaling [2]. Careful inspection of the data shows that, in identical stretching conditions, the gap $(\langle P_2(\cos\theta)\rangle_{MMA} - \langle P_2(\cos\theta)\rangle_S)$ is slightly larger for S-alt-M than for S-r-M. In addition, the relaxation rate of both S and MMA segments is lower for S-alt-M than for S-r-M. These results are consistent with the observations made on S-r-M copolymers containing variable amounts of S units [2].

4. Conclusions

On the example of the SM 50:50 alternating and random copolymers, this study shows in what manner the mechanical properties can be affected by the distribution of the two kinds of units along the chain. The results can be mainly interpreted in relation to the role of polar-polar intermolecular interactions between M units, which are likely to occur in the S-r-M copolymer, but are quite lacking in the S-alt-M copolymer. It is also shown that the influence of the triad MSM on the mechanical properties decreases progressively as long as the testing temperature approaches or exceeds T_α.

These conclusions are probably not specific to the case of the SM copolymers. They could be extended to the case of any copolymer prepared from the mixture of one non-polar monomer and one polar monomer, likely to promote strong dipolar interactions. It would also hold if one monomer is able to auto-associate itself by hydrogen bonding.

Acknowledgements

This study was supported by the Cultural, Scientific, and Technical Cooperation Department of the French Embassy in New Delhi (India), through a Post-Doctoral Grant in France, given to D. R.. Thanks are due to Dr Alain Polton and Dr Michel Tardi (Laboratoire de Chimie Macromoléculaire, Université Pierre et Marie Curie de Paris), who synthesized for us the S-alt-MMA copolymer. The authors are also indebted to Pierre Bertrand (Univ. of Ottawa) for the preparation of the figures.

References

1. J. L. HALARY, A. K. OULTACHE, J. F. LOUYOT, B. JASSE, T. SARRAF and R. MULLER, *J. Polym. Sci., Polym. Phys. Ed.* **29** (1991) 933.
2. A. K. OULTACHE, B. JASSE and L. MONNERIE, *ibid.* **32** (1994) 2539.
3. P. TORDJEMAN, J. L. HALARY, L. MONNERIE and A. M. DONALD, *Polymer* **36** (1995) 1627.
4. C. J. G. PLUMMER, H. H. KAUSCH, L. TEZE, J. L. HALARY and L. MONNERIE, *ibid.* **37** (1996) 4299.
5. P. TORDJEMAN, L. TEZE, J. L. HALARY and L. MONNERIE, *Polym. Eng. Sci.* **37** (1997) 1621.
6. L. TEZE, J. L. HALARY, L. MONNERIE and L. CANOVA, *Polymer* **40** (1999) 971.
7. Y. ZHAO, B. JASSE and L. MONNERIE, *Makromol. Chem., Macromol. Symp.* **5** (1986) 87; *idem. Polym. Commun.* **31** (1990) 395.
8. J. P. FAIVRE, Z. XU, J. L. HALARY, B. JASSE and L. MONNERIE, *Polymer* **28** (1987) 1881.
9. B. JASSE, J. F. TASSIN and L. MONNERIE, *Prog. Colloid Polym. Sci.* **92** (1993) 8; B. JASSE, *Trends Polym. Sci.* **3** (1993) 15.
10. B. JASSE, A. K. OULTACHE, H. MOUNACH, J. L. HALARY and L. MONNERIE, *J. Polym. Sci., Polym. Phys. Ed.* **34** (1996) 2007.
11. H. SUZUKI, Y. NISHIO, N. KIMURA, V. B. F. MATHOT, M. F. J. PIJPERS and Y. MURAKAMI, *Polymer* **35** (1994) 3698.
12. H. SUZUKI, N. KIMURA and Y. NISHIO, *ibid.* **35** (1994) 5555.
13. M. E. GALVIN, *Macromolecules* **24** (1991) 6354.
14. K. I. WINEY, M. L. BERBA and M. E. GALVIN, *ibid.* **29** (1996) 2868.
15. H. HIRAI, H. KOINUMA, T. TANABE and K. TAKEUCHI, *J. Polym. Sci., Polym. Chem. Ed.* **17** (1979) 1339.
16. A. M. AERDTS, J. W. DE HAAN and A. L. GERMAN, *Macromolecules* **26** (1993) 1965.
17. S. A. HEFFNER, F. A. BOVEY, L. A. VERGE, P. A. MIRAU and A. E. TONELLI, *Macromolecules* **19** (1986) 1628.
18. H. MOUNACH, thesis, Univ. P. M. Curie Paris, December 4, 1996.
19. J. D. FERRY, 'Viscoelastic Properties of Polymers' (3rd ed., John Wiley & Sons, New York, 1980).
20. A. K. DOOLITTLE and D. B. DOOLITTLE, *J. Appl. Phys.* **28** (1957) 901.
21. S. WU, *J. Polym. Sci., Polym. Phys. Ed.* **25** (1987) 2511; *idem.* **27** (1989) 723.
22. J. BRANDRUP and E. H. IMMERGUT, Eds, 'Polymer Handbook' (3rd ed., Wiley Interscience, New York, 1989).
23. S. WU and R. BECKERBAUER, *Polym. J.* **24** (1992) 1437.
24. I. M. WARD and D. H. HADLEY, 'Mechanical Properties of Solid Polymers' (John Wiley & Sons, New York, 1993).
25. J. HAUSSY, J. P. CAVROT, B. ESCAIG and J. M. LEFEBVRE, *J. Polym. Sci., Polym. Phys. Ed.* **18** (1980) 311.
26. J. M. LEFEBVRE and B. ESCAIG, *J. Mater. Sci.* **20** (1985) 438.
27. J. M. LEFEBVRE and B. ESCAIG, *Polymer* **34** (1993) 518.
28. I. M. WARD, 'Structure and Properties of Oriented Polymers' (Applied Science, London, 1975).
29. K. SCHMIDT-ROHR, A. S. KULIK, H. W. BECKHAM, A. OHLEMACHER, U. PAWELZIK, C. BOEFFEL and H. W. SPIESS, *Macromolecules* **27** (1994) 4733.
30. E. MUZEAU, J. PEREZ and G. P. JOHARI, *Macromolecules* **24** (1991) 4713.

31. J. M. GLOAGUEN, B. ESCAIG and J. M. LEFEBVRE, *J. Mater. Sci.* **30** (1995) 1111.
32. C. CRETON, J. L. HALARY and L. MONNERIE, *Polymer* **40** (1999) 199.
33. B. BRULE, J. L. HALARY and L. MONNERIE, *ibid.* **42** (2001) 9073.
34. D. RANA, V. SAUVANT and J. L. HALARY, *J. Mater. Sci.* **37** (2002) 5267.
35. A. DUBAULT, L. BOKOBZA, E. GANDIN and J. L. HALARY, *Polym. Int.* **52** (2003) 1108.

Received 26 February
and accepted 31 August 2004